angle and γ, which determines the fall off of the ionization with radius.

It is seen that η is not a sensitive function of these parameters. The geometry of the keep-alive contacts implies that θ_o tends to be rather small, typically $\theta_o \cong 20°$. The proper choice of γ can be estimated as follows: The electric field in the presence of a conical disturbance can be found as, [10]:

$$E \simeq \frac{E_o}{k_o r \sin\theta \ln(\cot(\theta_o/2))} \tag{14}$$

where k_o is the vacuum wave-number and E_o is the amplitude of the incident plane wave. As an average value of E we will use $E \simeq E_o/(k_o r)$. Furthermore, assuming $\nu_i \sim E^2$, cf. (2) and [9], we obtain $\nu_i = \alpha E^2 \equiv \nu_o a^2/r^2$, which implies $\nu_o a^2 = \alpha E_o^2/k_o^2$ and $\gamma = 1^+$.

The breakdown condition for $\theta_o = 20°$ and $\gamma = 1^+$ is then $\eta \approx 1$, i.e.

$$\frac{\nu_o a^2}{D} \simeq 1 \tag{15}$$

In fact, for an electric field given by (14), the ionization frequency depends on the angle θ as well as on the radius, r. For the case $\nu_i \sim E^2$, the ionization frequency becomes

$$\nu_i = \alpha E^2 = \frac{\alpha E_o^2}{k_o^2 \ln^2\left(\cot\frac{\theta_o}{2}\right)} \frac{1}{r^2 \sin^2\theta} \equiv \nu_o \frac{a^2}{r^2 \sin^2\theta} \tag{16}$$

The corresponding diffusion equation can be solved exactly to yield the eigenvalue

$$\eta = \frac{\pi}{2\left|\ln\tan\frac{\theta_o}{2}\right|} \cong 1 \tag{17}$$

in accordance with our previous estimate, (15). Thus, using (15) the following breakdown condition is obtained:

$$E_o \cong \left(\frac{k_o^2 D}{\alpha}\right)^{1/2} \tag{18}$$

which does not depend on the characteristic radius a.

In the experiments presented in [9], $k_o \simeq 2\,\mathrm{cm}^{-1}, \alpha \simeq 2 \cdot 10^2\,(\mathrm{V/cm})^{-2}\,\mathrm{s}^{-1}$ and D can be estimated as $D \simeq 10^5\,\mathrm{cm}^2/\mathrm{s}$, which implies $E_o \simeq 45$ V/cm. This corresponds to a power level of 2W at breakdown in good agreement with the observed level (1W). Furthermore, the characteristic distance, a, at which the ionization rate (and the field) saturates should be of the order of the distance between the truncated keep alive contacts (2a) in the TR-switch, i.e. $a \simeq 0.1$ mm. The maximum electric field enhancement is then obtained from (14) as $E/E_o \simeq 30$, again in good agreement with previous estimates, [9], [11].

The present analysis has considered in detail the problem of determining the threshold for breakdown in the strongly inhomogeneous electric field characteristic of microwave TR switches. The diffusion equation for the electron density has been solved exactly in the geometry of a double cone, which closely models the configuration of the breakdown region around the keep alive contacts in a TR switch. The analysis provides a significant step towards a self consistent determination of the breakdown threshold in microwave TR-switches. The predicted power levels for breakdown are shown to be in good agreement with previously published experimental results.

References

[1] A. D. Mac Donald, *Microwave Breakdown in Gases.* New York: Wiley, 1966.

[2] C. D. Maldonado and I. L. Ayala, "Diffusion-controlled breakdown of gases in cylindrical microwave cavity excited in the TM_{ono} mode," *J. Appl. Phys.*, vol. 43, p. 2650, 1972.

[3] J. T. Mayhan and R. L. Fante, "Microwave breakdown over a semi-infinite interval," *J. Appl. Phys.*, vol. 40, p. 5207, 1969.

[4] W. C. Taylor, W. E. Scharfman, and T. Morita, *Advances in Microwaves,* vol. 7, L. Young, Ed. New York: Academic, 1971.

[5] P. M. Platzman and E. H. Solt, "Microwave breakdown of air in nonuniform electric fields," *Phys. Rev.*, vol. 119, p. 1143, 1960.

[6] S. B. Cohn, "Rounded corners in microwave high-power filters and other components," *IRE Trans. Microwave Theory Tech.*, p. 389, 1961.

[7] A. S. Gilmour, Jr. *Microwave Tubes.* Dedham, MA: Artech House, 1986.

[8] V. B. Gildenburg and V. E. Semenov, "Theory of microwave breakdown of gases in nonuniform fields," *Sov. J. Plasma Phys.*, vol. 14, p. 292, 1988.

[9] M. Löfgren, D. Anderson, H. Bonder, H. Hamnén, and M. Lisak, "Breakdown phenomena in microwave transmit-receive switches," *J. Appl. Phys.*, vol. 69, 1981, 1991.

[10] M. Lisak, V. Semenov and D. Anderson, "Theory of electric field enhancement and power absorption in microwave transmit-receive switches," Report No. CTH-IEFT/PP-1992-01.

[11] W. Lipinski, M. Lisak, and D. Anderson, "Calculation of electric field enhancement in microwave TR-switches," Report No. CTH-IEFT/PP-1989-04 (unpublished).

Impedance, Attenuation and Power-Handling Characteristics of Double L-Septa Waveguides

Pradip Kumar Saha and Debatosh Guha

***Abstract*—Rectangular waveguides with two L-shaped septa attached to the broad walls in antipodal configuration have been shown theoretically to be an improved variant of the Double T-Septa Guide having larger cut off wavelength and broader bandwidth of the dominant TE mode [9]. Numerical data on the attenuation, impedance and power handling capability of this new type of broadband guides are now presented here as additional design information.**

I. Introduction

Recently we have proposed rectangular waveguides with shaped septa as new broadband transmission lines. The proposals were based on the results obtained from rigorous theoretical analysis of certain structures conceived intuitively. The first type of such guides has one or two T-shaped septa instead of the conventional ridges (Fig. 1(a)) to provide the necessary capacitive loading for increasing the modal separation [1]–[6]. Enhancement of bandwidth by dielectric loading of the septa gap was also determined theoretically [7], [8]. In the second type of proposed guides, the two septa are L-shaped and are attached to the broad walls in antipodal configuration (Fig. 1(b)). It has been designated the Double L-Septa Guide (DLSG). The results

Manuscript received October 8, 1991; revised August 28, 1992. This work was supported by the Council of Scientific and Industrial Research, India.

The authors are with Institute of Radio Physics and Electronics University of Calcutta, 92 A.P.C. Road, Calcutta-700 009 India.

IEEE Log Number 9207430.

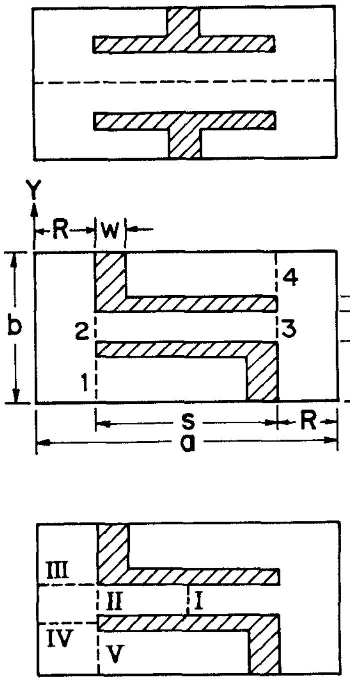

Fig. 1. (a) Double T-Septa Guide, bisection along the dotted line by an electric plane yields Single T-Septum Guide. (b) Double L-Septa Guide. Numbers 1–4 indicate the apertures referred to in Section II. (c) Double L-Septa Guide. I-V indicate the possible paths of the maximum transverse electric field.

of theoretical analysis of the DLSG indicate further improvement in the cut-off and bandwidth characteristics compared to those of the Double T-Septa Guide (DTSG) [9]. It has been shown that the DLSG also can have still broader range of these parameters when it is inhomogeneously loaded with dielectrics [10]. We have now determined theoretically the septa-gap impedance, attenuation and power handling capability of the dominant TE mode of the DLSG for a wide range of parameter values. These are presented here as design data and are compared with the DTSG and Double Ridged Guide (DRG).

II. Theory

The outline of the derivation of the matrix equation for determining the TE eigenvalue $k_c (= 2\pi/\lambda_c$ where λ_c is the cut-off wavelength) of the DLSG, using the Ritz–Galerkin technique, is given in [9]. The technique for computing the eigenvector corresponding to the dominant TE eigenvalue of the T-septa waveguides has been discussed in [2]. The same procedure is followed here for the DLSG for determining Z_{g_∞}, the impedance, on power-voltage basis, at the gap center at infinite frequency.

The power handling capability of the DLSG is determined by setting the maximum electric field in the guide equal to the breakdown field E_{bd} of the dielectric medium filling the guide and calculating the corresponding propagating power P_o. Then P_o represents the maximum power P_m that the DLSG can sustain. Here we consider $E_{bd} = 30$ KV/cm (unity safety factor) for an air-filled guide.

Following Zhang and Joines [4], we calculate the magnitude of the electric fields along the paths I, II, III, IV, V (Fig. 1(c)) where the electric field might assume the maximum value. For a particular set of septa parameters, the maximum of these field magnitudes is taken to calculate the corresponding maximum power flow.

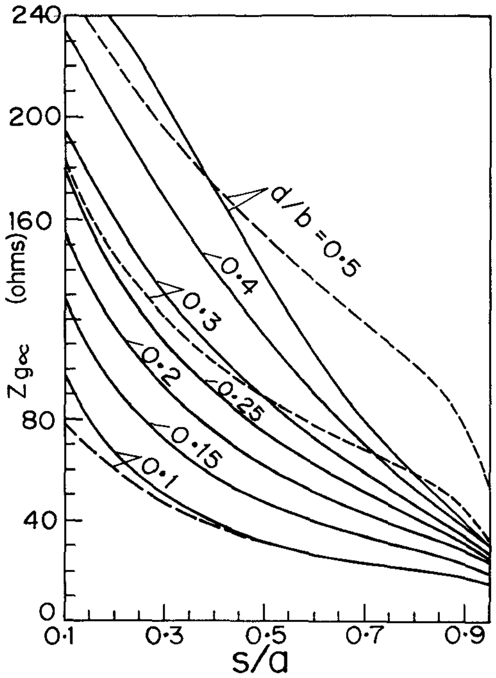

Fig. 2. Variation of gap impedance Z_{g_∞} with s/a. $b/a = 0.05$, $w/a = 0.1$, $t/b = 0.5$. —— DLSG. - - - - DTSG.

III. Numerical Results

The gap impedance Z_{g_∞} of the DLSG at the gap center as a function of the septa width s/a, with d/b as the parameter, is shown in Fig. 2. The corresponding data for the DTSG [2] for three values of d/b are shown in the figure for comparison. For small values of d/b the impedance characteristics of the two septa-guides are similar and they begin to differ significantly from $d/b \simeq 0.3$. For larger values of d/b, the gap impedance of the DLSG shows variation over wider range of values.

For presenting the theoretical attenuation characteristics of the dominant TE mode of the DLSG, we define a normalized attenuation coefficient α_n as the ratio of the attenuation coefficient α of the DLSG to that of a rectangular waveguide having identical TE_{10} cut-off frequency f_c. Fig. 3(a) shows the variation of α_n with s/a for various values of d/b. Also indicated are two attenuation curves of the DRG, which are derived, subject to the usual error, from Hopfer's [12] graphical data of α_n versus s/a for constant values of the bandwidth. One notes that as $s/a \to w/a (= 0.1$ here) and the DLSG degenerates into a DRG, there is difference between the present and Hopfer's data. The difference is small for large values of the gap width d/b but for small values of d/b this discrepancy is large. For example, at $d/b = 0.1$, Hopfer's value of α_n of the DRG is about 13 while the present method yields a value of about 8. Zhang and Joines [4] have also reported similar discrepancy between their and Hopfer's value of α_n of the single ridged guide. Fig. 3(a) also shows that α_n (DLSG) increases monotonically with s/a for a fixed d/b and when compared to the apparently overestimated values for Hopfer, it remains lower than α_n (DRG) for $s/a < 0.6$. The absolute attenuation coefficient of the DLSG, normalized as $\alpha a/\sqrt{f}$, is shown in Fig. 3(b) as a function of f/f_c. Some results are also included in the figure to show that the effect of small change in the septa thickness on the attenuation is not significant.

Fig. 4 shows the theoretical power handling capability of the DLSG in the form of P_m/λ_c^2 as a function of s/a with d/b as the parameter. The calculations do not take into account the possible electric field singularity at sharp corners. This aspect has been discussed by Hopfer

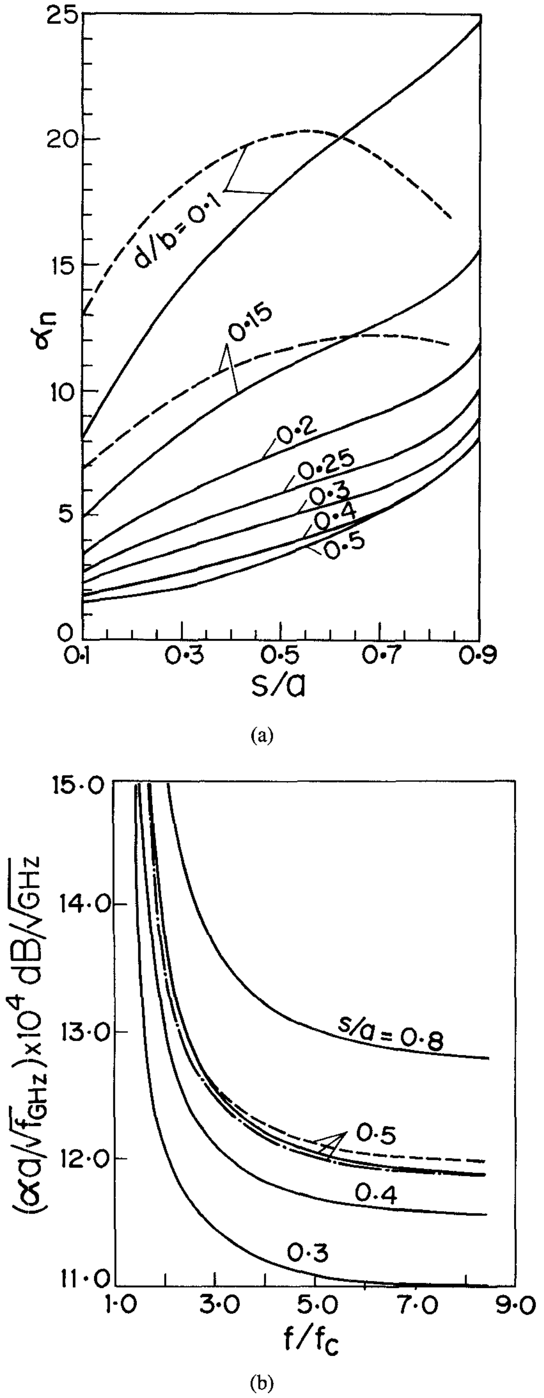

Fig. 3. (a) Theoretical attenuation characteristics. Normalized attenuation coefficient α_n versus s/a at $f = \sqrt{3}f_c$. $b/a = 0.5, w/a = 0.1, t/b = 0.05$. {—}{—} DLSG. - - - DRG. (b) Theoretical attenuation characteristics of DLSG. Normalized attenuation coefficient $\alpha a/\sqrt{f}$ versus f/f_c. Material: copper. $b/a = 0.5, d/b = 0.3$. {—}{—} $w/a = 0.1, t/b = 0.05$ - - - $w/a = 0.1, t/b = 0.01$ -.-.-.-.-. $w/a = 0.2, t/b = 0.05$.

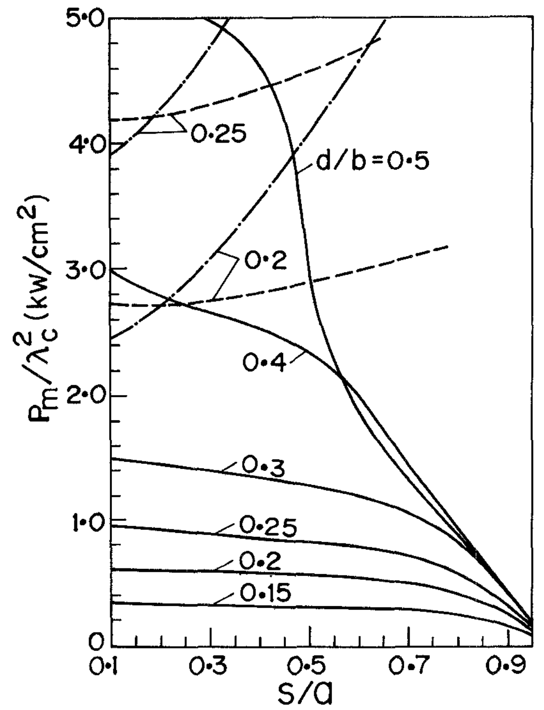

Fig. 4. Theoretical power handling capability of DLSG: P_m/λ_c^2 versus s/a. $b/a = 0.5, w/a = 0.1, t/b = 0.05$. The dotted curves are the characteristics for breakdown in the gap center only. {—}{—} DLSG. -.-.-.-.-. DRG.

[12] in connection with ridged waveguides. In the case of DLSG an estimation of the edge effect itself would require a separate calculation because of the complexity of the structure. However, such singularities can be avoided in practice by slight rounding off of the sharp corners. Nevertheless, certain features which emerge from our computed results are worth mentioning.

If we presume that the power handling characteristics of the DTSG would not be much different in nature from the STSG characteristics calculated by Zhang and Joines [4], we observe that the DLSG characteristics are significantly different. The DLSG power handling capability also appears to be poor, in comparison with SRG [12] and T-septa guide [4]. The DRG curves in Fig. 4 were computed from Hopfer's expression in [12]. The comparison, however, should be made cautiously because the available ridged and T-septa waveguide data have certain limitations. Hopfer's calculations on the ridged guides are based on the breakdown at the ridge-gap-center while he points out that the electric field is actually stronger at the gap edges [12]. The data of STSG in [4] are also based on the field at the gap center and on the field between the septa edges and the side walls when the septa width is large. However, in the T-septa guides also, the electric field at the septa-gap-edges is always stronger than at the center. Thus, if the correct electric field distribution in the gap is taken into account, the theoretical power handling capability of the STSG would be poorer than that reported in [4]. Similarly, Hopfer's calculation also overestimates the breakdown power level in the ridged guides. To illustrate this point we present two broken-line curves in Fig. 4 which are obtained as the power handling characteristics of the DLSG if breakdown occurs only in the gap center. The curves are not only similar to the DRG characteristics, but also show comparable values of P_m/λ_c^2.

Our calculations show that the breakdown in the DLSG would never occur at the gap center because the electric field there is never the strongest, but may occur along one of the three paths II, IV and V (Fig. 1(c)) depending on the values of d/b and s/a. For example, in Fig. 4, the power handling curve for $d/b = 0.3$ relates to the breakdown at the gap edges (path II) for all values of s/a up to 0.9 after which the path IV takes over. At smaller values of d/b the breakdown occurs only at the gap edges for all values of s/a. At $d/b = 0.4$, the breakdown occurs at the gap edges for $s/a \leq 0.5$. For $s/a > 0.5$, the field along the path V at the back of the septa determines the breakdown power level. Finally, for $s/a > 0.9$, the breakdown shifts to the path IV. This pattern of breakdown, however, changes completely for $d/b = 0.5$. For small values of the septa width s/a, the P_m/λ_c^2 now corresponds to the breakdown along the path V and decreases rapidly. For $s/a \simeq 0.4$ the breakdown shifts to the gap edges (path II) and P_m/λ_c^2 drops sharply. Then for $s/a > 0.4$, the electric field at the septa edges (path IV) becomes the dominant factor in determining the breakdown power level. Whatever be the region of breakdown in the DLSG, P_m/λ_c^2 increases rapidly with increasing gap width d/b for $s/a < 0.5$. The power level also decreases monotonically with increasing s/a—very slowly when d/b is small and more rapidly for larger values of d/b.

IV. Conclusions

We have reported earlier that a Double L-Septa Guide has better cut-off and bandwidth characteristics than a Double T-Septa Guide [9], [10]. We have now extended the theoretical study of the DLSG by calculating the attenuation characteristics, septa-gap impedance and power handling capability of the dominant TE mode of the guide. The design data are presented for a wide range of septa parameters. These characteristics compare favorably with those of the ridged and T-septa guides and, together with the superior bandwidth, should make the DLSG a useful broadband transmission medium.

References

[1] G. G. Mazumder and P. K. Saha, "A novel rectangular waveguide with double T-septums," *IEEE Trans. Microwave Theory Tech.*, vol. MTT-33, pp. 1235–1238, Nov. 1985.

[2] ——, "Rectangular waveguide with T-shaped septa," *IEEE Trans Microwave Theory Tech.*, vol. MTT-35, pp. 201–204, Feb. 1987.

[3] Y. Zhang and W. T. Joines, "Some properties of T-septum waveguides," *IEEE Trans. Microwave Theory Tech.*, vol. MTT-35, pp. 769–775, Aug. 1987.

[4] Y. Zhang and W. T. Joines, "Attenuation and power-handling capability of T-septum waveguides," *IEEE Trans. Microwave Theory Tech.*, vol. MTT-35, pp. 858–861, Sept. 1987.

[5] F. J. German and L. S. Riggs, "Bandwidth properties of rectangular T-septum waveguides," *IEEE Trans. Microwave Theory Tech.*, vol. MTT-37, pp. 917–919, May 1989.

[6] B. E. Pauplis and D. C. Power, "On the bandwidth of T-septum waveguides," *IEEE Trans. Microwave Theory Tech.*, vol. MTT-37, pp. 919–922, May 1989.

[7] G. G. Mazumder and P. K. Saha, "Bandwidth characteristics of inhomogeneous T-septum waveguides," *IEEE Trans Microwave Theory Tech.*, vol. 37, pp. 1021–1026, June 1989.

[8] R. R. Mansour and R. H. Macphie, "Properties of dielectric loaded T-septum waveguides," *IEEE Trans Microwave Theory Tech.*, vol. 37, pp. 1654–1657, Oct. 1989.

[9] P. K. Saha and D. Guha, "New broadband rectangular waveguide with L-shaped septa," *IEEE Trans. Microwave Theory Tech*, vol. 40, pp. 777–781, Apr. 1992.

[10] P. K. Saha and D. Guha, "Characteristics of inhomogeneously filled double L-septa waveguides," *IEEE Trans. Microwave Theory Tech.*, Nov. 1992.

[11] R. E. Collin, "Field Theory of Guided Waves. New York: McGraw-Hill, 1960.

[12] S. Hopfer, "The design of ridged waveguides," *IRE Trans. Microwave Theory Tech.*, vol. MTT-3, pp. 20–29, Oct. 1955.

On the Use of Levin's T-Transform in Accelerating the Summation of Series Representing the Free-Space Periodic Green's Functions

Surendra Singh and Ritu Singh

Abstract—**The Levin's t-transform is shown to accelerate the summation of slowly converging series. This is illustrated by application of the transform to the series representing the free-space periodic Green's functions involving a single and double infinite summation. Numerical results indicate that the transform converges rapidly than a direct summation of the series. Thus, it provides considerable savings in computation time.**

I. Introduction

The series representing the free-space periodic Green's function converges very slowly. This slow convergence results in making the analysis of periodic structures computationally expensive. In order to improve the efficiency of the codes, it is essential to employ methods to enhance the convergence of the Green's function series. Recently, a number of investigators [1]–[3] have used methods to reduce the computation time by a considerable amount. In this work, we show that the use of Levin's t-transform [4] is able to accelerate the summation of slowly converging series involving a single and double infinite summation. The primary advantage of the transform is that it is relatively free of roundoff errors in the computation of higher order iterates. In addition to this the transform can be applied to any slowly converging series without performing any analytical work prior to its application. The transform is outlined in Section II with an illustrative example. In Section III, the free-space periodic Green's functions are given. The numerical results and conclusion are presented in Sections IV and V, respectively.

II. Levin 's t-Transform

Let S_n be the partial sum of n terms of a series such that $S_n \rightarrow S$ as $n \rightarrow \infty$, where S is the sum of the series. The Levin's t-transform may be computed as follows:

$$t_k^{(n)} = \frac{\displaystyle\sum_{i=0}^{k}(-1)^i\binom{k}{i}\left(\frac{n+i}{n+k}\right)^{(k-1)}\left(\frac{S_{n+i}}{S_{n+i+1}-S_{n+i}}\right)}{\displaystyle\sum_{i=0}^{k}(-1)^i\binom{k}{i}\left(\frac{n+i}{n+k}\right)^{(k-1)}\left(\frac{1}{S_{n+i+1}-S_{n+i}}\right)},\quad k = 0, 1, 2, \cdots \tag{1}$$

The kth order transform, $t_k^{(n)}$ or $t_k(S_n)$, gives an estimate of the sum, S, of the series. An inherent advantage of the t-transform is that the higher order iterates are computed from the partial sums. Hence, the accuracy to which the partial sums are computed can be preserved in the transform computations. This keeps the transform relatively immune to roundoff errors in comparison to Shanks' transform [5] in which higher order iterates are computed from the lower orders resulting in severe loss of significant digits due to accumulation of roundoff errors [6]. The transform can be illustrated by applying it

Manuscript received November 19, 1991; revised September 15, 1992.
The authors are with Department of Electrical Engineering, The University of Tulsa, Tulsa, Oklahoma 74104.
IEEE Log Number 9207404.